Optimal control of coupled spins in the presence of longitudinal and transverse relaxation

Dionisis Stefanatos* and Navin Khaneja†
Division of Applied Sciences, Harvard University, Cambridge, Massachusetts 02138, USA

Steffen J. Glaser‡
Institute of Organic Chemistry and Biochemistry II, Technische Universität München, 85747 Garching, Germany
(Received 13 August 2003; published 26 February 2004)

In this paper, we develop methods for optimal manipulation of coupled spin dynamics in the presence of relaxation. These methods are used to compute analytical bounds for the optimal efficiency of coherence transfer between coupled nuclear spins in presence of longitudinal and transverse relaxation. We derive relaxation optimized pulse sequences which achieve these bounds and maximize the sensitivity of the experiments in spectroscopic applications. This paper is a continuation of our previous work. Here, we take into account both the longitudinal and the transverse relaxation mechanisms, thus generalizing our previous results, where the former had been neglected.

DOI: 10.1103/PhysRevA.69.022319 PACS number(s): 03.67.−a, 03.65.Yz, 82.56.Jn, 82.56.Fk

I. INTRODUCTION

In applications involving control and manipulation of quantum phenomena, the system of interest is not isolated but interacts with its environment. This leads to the phenomenon of relaxation, which in practice results in signal loss and ultimately limits the range of applications. Manipulating quantum systems in a manner that minimizes relaxation losses poses an important practical problem. A premier example is the transfer of coherence between coupled spins in NMR spectroscopy [1]. Presence of relaxation limits the efficiency of coherence transfer between coupled spins and results in poor sensitivity of the experiments. The problem becomes pronounced in NMR spectroscopy of large biomolecules. With increasing size of molecules or molecular complexes, the rotational tumbling of the molecules becomes slower and leads to increased relaxation losses. When these relaxation rates become comparable to the spin-spin couplings, the efficiency of coherence transfer is considerably reduced, leading to poor sensitivity and significantly increased measurement times.

This negative effect of relaxation on the efficiency of coherence transfer automatically gives rise to some important practical (and theoretical) problems.

(1) What is the theoretical upper limit for the coherence transfer efficiency in the presence of relaxation?

(2) How can this theoretical upper limit be reached experimentally?

In our previous work, we answered the above questions for a coupled two-spin system under the presence of transverse relaxation [2,3] (neglecting and including cross-correlation effects, respectively). In this manuscript, we extend these results to the case where both longitudinal and transverse relaxation mechanisms are important, and we cannot neglect the former.

The methods developed here are also useful for answering important questions in quantum information theory. It is a fundamental problem to understand the extent to which an open quantum system can be controlled, i.e., where all the state of a quantum-mechanical system can be steered in the presence of relaxation? How much entanglement can be produced in presence of decoherence and dissipation and what is the optimal way to synthesize unitary gates in open quantum systems so as to maximize their fidelity? All these problems are related to optimal control of quantum-mechanical systems in presence of relaxation.

II. RELAXATION IN NMR IN LIQUIDS

As a model system, we consider optimal control of ensembles of nuclear spins in NMR spectroscopy. We use ρ to denote the density matrix for the spin ensemble. The density matrix of a closed quantum system ($\hbar=1$) evolves as

$$\frac{d\rho}{dt}=-i[H(t),\rho], \tag{1}$$

where $H(t)$ is the Hamiltonian of the system.

For an open quantum system, the evolution is no longer unitary. In many applications of interest, the environment can be approximated as an infinite thermostat, whose own state never changes. Under this assumption, also called the Markovian approximation, it is possible to write the evolution of the density matrix of the system (master equation) alone in the (Lindblad) form [4]

$$\frac{d\rho}{dt}=-i[H(t),\rho]+L(\rho), \tag{2}$$

where the term $L(\rho)$ is linear in ρ and models relaxation. The general form of L is

*Electronic address: stefanat@fas.harvard.edu
†Electronic address: navin@hrl.harvard.edu.;
URL: http://hrl.harvard.edu/~navin
‡URL: http://ociialf.org.chemie.tu-muenchen.de/glaser

$$L(\cdot)=\sum_{\alpha,\beta} J_{\alpha\beta}[V_\alpha,[V_\beta^\dagger,\cdot]], \tag{3}$$

where $V_{\alpha,\beta}$ are operators that represent various relaxation mechanisms and $J_{\alpha\beta}$ are coefficients that depend on the physical parameters of the problem.

Our focus in this paper is on the relaxation phenomena in the liquid state NMR spectroscopy. In this case, the system is modeled as being composed of two weakly interacting parts: the spin system, consisting of all spin degrees of freedom of the nuclei, and the lattice, consisting of all other degrees of freedom of the liquid sample, associated with the molecular rotations and translations. Molecules in solution are constantly being bombarded with solvent molecules and undergo random ''Brownian'' motion as a result. This stochastic Brownian motion is the principle mechanism of relaxation in NMR spectroscopy. The small intercollision time of the order of 10^{-12}–10^{-14} sec, ensures that the correlations between the spin system and the heat bath decay much faster than the evolution of the spin system and thus a Markovian approximation is a valid assumption.

Note that, since we consider classical motion of the molecules (rotations and translations), we adopt the so-called semiclassical approximation, where the spin system is treated quantum mechanically and the lattice is treated classically [5,6]. Specifically, the Hamiltonian for the system is written as the sum of a deterministic Hamiltonian H_0, which acts only on the spin system, and a stochastic Hamiltonian $H_1(t)$, which couples the spin system to the lattice:

$$H=H_0+H_1(t). \tag{4}$$

For our purposes, we consider H_0 time independent. The Hamiltonian $H_1(t)$ is a random function of time and we assume that it has a vanishing average value. If it is not, we can incorporate the average value to H_0, so the resulting $H_1(t)$ has a zero average. The stochastic Hamiltonian has to do with the relaxation phenomena and can be written in the form

$$H_1(t)=\sum_\alpha V_\alpha F_\alpha(t), \tag{5}$$

where the V_α are spin operators (the relaxation operators defined above) and the $F_\alpha(t)$ are random functions of time.

To demonstrate the basic principles, we examine an isolated pair of heteronuclear spins I and S (spins that belong to different nuclear species) with indirect interaction (mediated by the surrounding electrons). For such a system, the deterministic Hamiltonian H_0 is given in [6]

$$H_0=H_Z+H_{ind}, \tag{6}$$

where H_Z is the Zeeman Hamiltonian for the spins I and S,

$$H_Z=\omega_I I_z+\omega_S S_z, \tag{7}$$

and H_{ind} is the Hamiltonian for the indirect interaction between them. The general form of H_{ind} for two spins is

$$H_{ind}=\boldsymbol{I}\cdot\boldsymbol{J}\cdot\boldsymbol{S}, \tag{8}$$

where $\boldsymbol{J}$ is a tensor. The only effective part of this interaction in liquids is its average over all relative orientations of the spins in space. In isotropic liquids it is of the form

$$H_{ind}=2\pi J\boldsymbol{I}\cdot\boldsymbol{S}, \tag{9}$$

where J is the scalar coupling constant. In the weak-coupling limit ($J\ll|\omega_I-\omega_S|$), the indirect interaction Hamiltonian is simplified to the form [6]

$$H_{ind}=2\pi J I_z S_z. \tag{10}$$

For heteronuclear spins I and S the weak-coupling condition is always satisfied. Thus, the deterministic Hamiltonian for our system is

$$H_0=\omega_I I_z+\omega_S S_z+2\pi J I_z S_z. \tag{11}$$

We now go to an intermediate representation defined by the operator

$$U=\exp(iH_Z t)=\exp[i(\omega_I I_z+\omega_S S_z)t]. \tag{12}$$

Observe that this representation corresponds to a doubly rotating frame (a frame rotating with different frequency for each spin). Let

$$\tilde{\rho}=U\rho U^\dagger. \tag{13}$$

In this intermediate representation, the initial equation $\dot{\rho}=-i[H,\rho]$ becomes

$$\frac{d\tilde{\rho}}{dt}=-i\pi J[2I_z S_z,\tilde{\rho}]-i[\tilde{H}_1(t),\tilde{\rho}]. \tag{14}$$

Let τ_c be the correlation time of the random functions $F(t)$ defined above, i.e., it is the time scale $t-t'=\tau_c$ over which a typical product $F_\alpha(t)F_\beta^*(t')$ decays by a substantial amount. Following the standard procedure described in Ref. [7] and using that (1) the evolution through relaxation of the physical variables under study is slow on the time scale τ_c (this is the Markovian approximation and has been justified for our spin system in a previous paragraph) and (2) the fact that $J^{-1}\gg\tau_c$ (the correlation time τ_c is of the order of nanoseconds [8], while the inverse coupling constant J^{-1} is of the order of milliseconds [2]), we end up with the master equation

$$\frac{d\sigma}{dt}=-i\pi J[2I_z S_z,\sigma]+L(\sigma-\sigma_{eq}). \tag{15}$$

Here σ is the reduced density matrix for the spin system, i.e., the average of the previous $\tilde{\rho}$ over the lattice degrees of freedom. So $\sigma=\overline{\tilde{\rho}}$, where the bar denotes this average. The thermal equilibrium value of σ is denoted by σ_{eq}. The form of the relaxation superoperator L for our system is given in the following paragraphs.

TABLE I. Relaxation operators for DD and CSA interactions. We have used the standard notation $I^{\pm}=I_x \pm iI_y$.

V_α^{DD}	$\frac{2}{\sqrt{6}}I_zS_z$	$-\frac{1}{2\sqrt{6}}I^+S^-$	$-\frac{1}{2}I_zS^+$	$-\frac{1}{2}I^+S_z$	$\frac{1}{2}I^+S^+$
		$-\frac{1}{2\sqrt{6}}I^-S^+$	$\frac{1}{2}I_zS^-$	$\frac{1}{2}I^-S_z$	$\frac{1}{2}I^-S^-$
V_β^{CSA}	$\frac{2}{\sqrt{6}}I_z$	$-\frac{1}{2}I^+$	$\frac{1}{2}I^-$		

In NMR spectroscopy in liquid solutions, the most important relaxation mechanisms are due to dipole-dipole (DD) interaction and chemical shift anisotropy (CSA), as well as their interference effects (DD-CSA cross-correlation terms) [9,10]. We describe briefly these relaxation mechanisms.

Any magnetic nucleus in a molecule generates an instantaneous magnetic dipolar field that is proportional to the magnetic moment of the nucleus. This field interacts with the magnetic moments of the nearby magnetic nuclei. As the molecule tumbles in solution, the field fluctuates and constitutes a mechanism for relaxation of the nearby spins. For isotropic distribution of the interaction orientation in space, which is the case for liquid solutions, the average value of the dipolar interaction vanishes. That is why the (direct) dipole-dipole interaction does not give any contribution to the deterministic (static) Hamiltonian H_0, while the indirect interaction (mediated through the electrons) gives. The dipole-dipole interaction contributes only to the stochastic Hamiltonian $H_1(t)$.

We mentioned above that the indirect interactions between spins are mediated through the electrons. The magnetic field, produced by the magnetic moment of one spin, modifies the electronic ground state in such a way that the electronic system achieves a small magnetization proportional to that field (note that the great majority of NMR experiments is performed on nuclear spins of atoms belonging to diamagnetic molecules, in which the orbital and spin angular momenta of the individual electrons are coupled in such a way that their bulk angular momentum and magnetic moment both vanish). This electronic magnetization produces a small extra magnetic field that changes the magnetic field experienced by the other spin. By the same means, the static external magnetic field, which gives the Zeeman terms in H_0, modifies the electronic environment and changes the magnetic field experienced by the spins. The resulting interaction has a nonvanishing average value, which is incorporated in H_0 as a change in the Zeeman frequencies ω_I, ω_S and is called the chemical shift. The remaining part is incorporated in $H_1(t)$. This part gives the chemical shift anisotropy relaxation mechanism (the term anisotropy is used to emphasize that it corresponds to the anisotropic part of the interaction, which is present because the electronic environment of a nucleus is not isotropic in general).

The relaxation operators V_α, corresponding to DD and CSA relaxation mechanisms, can be found in Ref. [8] and are given in Table I. If we ignore the interference effects between these two mechanisms (cross-correlated relaxation), the relaxation superoperator L for our system can be written as the sum of two terms, each of which corresponds to one relaxation mechanism. It is

$$L(\cdot)=\sum_\alpha J_\alpha[V_\alpha^{DD},[V_\alpha^{DD\dagger},\cdot]]+\sum_\beta J_\beta[V_\beta^{CSA},[V_\beta^{CSA\dagger},\cdot]], \tag{16}$$

where the coefficients J_α, J_β depend on the physical parameters of the system, such as the gyromagnetic ratios of the spins, the internuclear distance, the correlation time of the molecular tumbling, and the anisotropy of the chemical shift tensor.

Having found the relaxation superoperator L for our system, we can use the master equation (15) to derive evolution equations for the ensemble averages of the operators that we are interested in. Doing so, we find that the operator I_z evolves according to the equation

$$\frac{d\langle I_z\rangle}{dt}=-\pi k_1(\langle I_z\rangle-I_0)-\pi k_{cr}(\langle S_z\rangle-S_0), \tag{17}$$

where k_1 is the longitudinal self-relaxation rate for I_z, k_{cr} is the longitudinal cross-relaxation rate between the spins I and S, and I_0, S_0 are the equilibrium values for $\langle I_z\rangle, \langle S_z\rangle$, respectively. The relaxation rates k_1 and k_{cr} are functions of the coefficients J_α, J_β, thus depending on the same physical parameters. They are given explicitly in Ref. [8]. For heteronuclear spins I and S, we ignore the (small) cross relaxation between spins I and S, i.e., we set $k_{cr}=0$ (this approximation is very good for large molecules where $\tau_c^{-1}\ll|\omega_I-\omega_S|$). The above equation becomes

$$\frac{d\langle I_z\rangle}{dt}=-\pi k_1(\langle I_z\rangle-I_0). \tag{18}$$

In general, polarization $\langle I_z\rangle$ relaxes towards its thermal equilibrium polarization I_0. For example, this thermal correction must be taken into account in transfer steps that are applied in the preparation period of an experiment [1]. However, if coherences of some nonzero order are selected at a given point in the pulse sequence using phase cycles or magnetic-field gradients, the thermal correction can be omitted from all subsequent pulse sequence elements [11]. Here, we focus on this case, which corresponds, e.g., to all *mixing steps* in multidimensional NMR experiments which are always applied after an evolution period in which a nonzero coherence order is selected. Hence, we can set $I_0=0$ and Eq. (18) is reduced to

$$\frac{d\langle I_z\rangle}{dt}=-\pi k_1\langle I_z\rangle. \tag{19}$$

The operator I_x evolves under the J coupling to $2I_yS_z$ and also relaxes with rate k (transverse relaxation),

$$\frac{d\langle I_x\rangle}{dt}=-\pi J\langle 2I_yS_z\rangle-\pi k\langle I_x\rangle. \tag{20}$$

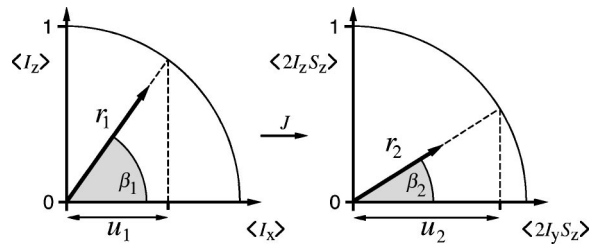

FIG. 1. Representation of the system variables r_1, r_2, the angles β_1, β_2, and of the control parameters $u_1 = \cos\beta_1, u_2 = \cos\beta_2$ in terms of the expectation values $\langle I_x\rangle, \langle I_z\rangle, \langle 2I_yS_z\rangle, \langle 2I_zS_z\rangle$.

As the operator $2I_yS_z$ is produced, it also relaxes with rate k. This is a very good approximation for many systems. In general the transverse operators I_x and $2I_yS_z$ may relax at different rates. However the methods presented can be easily extended to account for this case. The operator $2I_zS_z$ relaxes with rate k_2 (longitudinal relaxation),

$$\frac{d\langle 2I_zS_z\rangle}{dt} = -\pi k_2\langle 2I_zS_z\rangle, \tag{21}$$

$$\frac{d\langle 2I_yS_z\rangle}{dt} = \pi J\langle I_x\rangle - \pi k\langle 2I_yS_z\rangle. \tag{22}$$

The rates k and k_2 depend on the same parameters as k_1.

In this paper, we address the problem of finding the maximum efficiency for the transfers

$$I_\alpha \rightarrow 2I_\beta S_\gamma \tag{23}$$

and

$$I_\alpha \rightarrow S_\beta, \tag{24}$$

where α, β, and γ can be x, y, or z. These transfers are of central importance for two-dimensional NMR spectroscopy and are conventionally accomplished by the INEPT [12] and refocused INEPT [13] pulse sequence elements, respectively. We describe INEPT (insensitive nuclei enhanced by polarization transfer) in the following section and formulate our problem in terms of optimal control theory.

III. FORMULATION OF THE PROBLEM IN TERMS OF OPTIMAL CONTROL

The two heteronuclear spins have well separated frequencies, allowing for fast selective manipulation of each spin on a time scale determined by the coupling J and the relaxation rates k, and k_1 or k_2. Thus, the Cartesian spin operator I_α can be transformed to an operator of the form $I_x\cos\beta_1 + I_z\sin\beta_1$ by the use of strong, spin selective radio-frequency (rf) pulses without relaxation losses (see Fig. 1). Let $r_1(t)$ represent the magnitude of polarization and in phase coherence on spin I at any given time t, i.e., $r_1(t) = \sqrt{\langle I_x\rangle^2 + \langle I_z\rangle^2}$. Using rf fields, we can exactly control the angle β_1. So, we can think of $\cos\beta_1$ as a control parameter and denote it by u_1 (see Fig. 1).

In the same manner, by the use of rf pulses, it is possible to rotate the operator $2I_yS_z$ to $2I_zS_z$. Let $r_2(t)$ represent the total magnitude of the expectation values of these bilinear operators, i.e., $r_2(t) = \sqrt{\langle 2I_yS_z\rangle^2 + \langle 2I_zS_z\rangle^2}$. We can control the angle β_2 (Fig. 1) and we define $\cos\beta_2$ as a second control parameter u_2. Using the equations for the ensemble averages, given in the preceding section, we find

$$\frac{d}{dt}\begin{bmatrix} r_1 \\ r_2 \end{bmatrix} = A(\cos\beta_1, \cos\beta_2)\begin{bmatrix} r_1 \\ r_2 \end{bmatrix}, \tag{25}$$

where

$$A(\cos\beta_1, \cos\beta_2) = \pi J\begin{bmatrix} -\frac{k-k_1}{J}\cos^2\beta_1 - \frac{k_1}{J} & -\cos\beta_1\cos\beta_2 \\ \cos\beta_1\cos\beta_2 & -\frac{k-k_2}{J}\cos^2\beta_1 - \frac{k_2}{J} \end{bmatrix}. \tag{26}$$

Let

$$\xi_1 = \frac{k-k_1}{J}, \quad \overline{\xi_1} = \frac{k_1}{J}, \quad \xi_2 = \frac{k-k_2}{J}, \quad \overline{\xi_2} = \frac{k_2}{J} \tag{27}$$

and rescale the time according to $t_{new} = \pi J t_{old}$. Using $u_1 = \cos\beta_1$, $u_2 = \cos\beta_2$, we find the following equation for r_1, r_2 (by abuse of notation we use the same t for the new time):

$$\frac{d}{dt}\begin{bmatrix} r_1 \\ r_2 \end{bmatrix} = \begin{bmatrix} -\xi_1 u_1^2 - \overline{\xi_1} & -u_1u_2 \\ u_1u_2 & -\xi_2 u_2^2 - \overline{\xi_2} \end{bmatrix}\begin{bmatrix} r_1 \\ r_2 \end{bmatrix}. \tag{28}$$

The initial conditions are

$$r_1(0) = 1, \quad r_2(0) = 0. \tag{29}$$

Note that starting from the ensemble average equations, we brought the system equations in a form where the principles of optimal control can be applied. The problem that we face is as follows: given the dynamical system above, how should $u_1(t), u_2(t)$, with $0 \leqslant u_1, u_2 \leqslant 1$, be chosen so that starting from $r_1(0) = 1$ we achieve the largest value $r_2(T)$ for a specified finite time T. In spectroscopic applications this would correspond to the maximum efficiency for the transfer of I_α to $2I_\beta S_\gamma$. This transfer is conventionally accomplished by the INEPT pulse sequence: At time $t = 0$ we apply a hard pulse which rotates I_α to I_x. Then, we let this operator evolve under the J coupling towards $2I_yS_z$ for the whole time interval $[0,T]$, i.e., we keep $\beta_1 = \beta_2 = 0$ $[u_1(t) = u_2(t) = 1]$ during this interval. Finally, by applying the appropriate hard pulses at $t = T$, we rotate the operator $2I_yS_z$ to $2I_\beta S_\gamma$. Schematically, the INEPT pulse sequence is

$$I_\alpha \rightarrow I_x \dashrightarrow 2I_yS_z \rightarrow 2I_\beta S_\gamma,$$

where the solid arrow represents hard pulses, while the dashed arrow represents the evolution under the J coupling. In this manuscript we prove that in the presence of relaxation, this is not in general the optimal procedure. Having found the optimal controls $u_1(t), u_2(t)$, we can calculate the

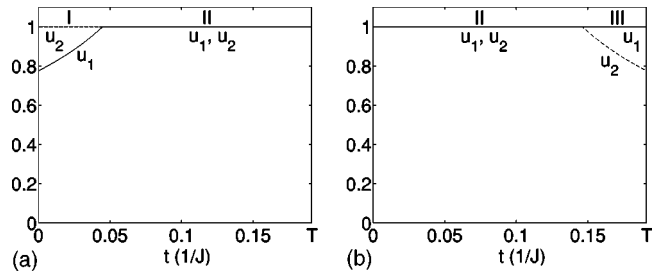

FIG. 2. Optimal pulse sequence when $T_A<T\leqslant T_B$ for (a) $k_1<k_2$ and (b) $k_1>k_2$. For case (b) we just interchanged the values of k_1,k_2 from case (a), keeping the same k. Observe the symmetry in the optimal controls.

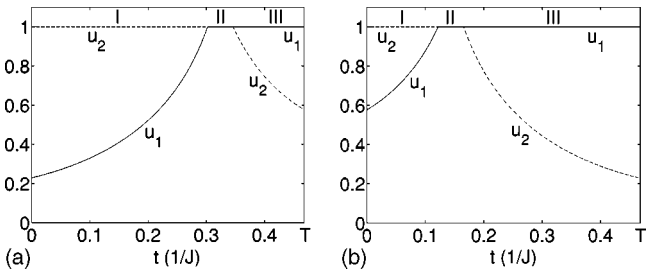

FIG. 3. Optimal pulse sequence when $T>T_B$ for (a) $k_1<k_2$ and (b) $k_1>k_2$. Again, for case (b) we just interchanged the values of k_1,k_2. The symmetry in the controls appears again. Note that the duration T has been set equal to the optimal duration T_{opt}, which maximizes the optimal transfer efficiency η_T. For the values $k=J,k_1=0.05J,k_2=0.25J$ that we used in (a), it is $T_{opt}\simeq 0.468J^{-1}$. For case (b), T_{opt} is the same.

corresponding magnetic-field components $B_x(t),B_y(t)$, which achieve the maximum efficiency.

IV. THEORETICAL RESULTS

The optimal control problem is solved in Appendix A. Here, we describe the characteristics of the optimal pulse sequence for the case $\xi_1>\xi_2$, i.e., for $k_1<k_2$. The results for $k_1>k_2$ are analogous. Presence of finite longitudinal relaxation rates results in an optimal transfer duration T_{opt} in which the maximum transfer efficiency is achieved. We compute this T_{opt} by finding the optimal pulse sequence for every choice of transfer duration T and then locating the T that gives the best transfer efficiency. Depending on the values of the problem parameters, we find three important cases in the optimal solution.

(1) $T\leqslant T_A$ (case A) [$T_A=\cot^{-1}(2\xi_1)/\pi J$, for $\xi_1>\xi_2$]: In this case $u_1(t)=u_2(t)=1$ throughout, i.e., β_1 and β_2 in Fig. 1 are always kept zero and this solution corresponds to the INEPT pulse sequence.

(2) $T_A<T\leqslant T_B$ (case B1) (we describe how we calculate T_B below): In this case the optimal pulse sequence has two distinct phases [see Fig. 2(a)]. There is a switching time τ_1 such that for $0\leqslant t\leqslant\tau_1$ (phase I), $u_2(t)=1$ and $u_1(t)$ is increased gradually from a value $u_1(0)<1$ to $u_1(\tau_1)=1$. Then, for time $\tau_1\leqslant t\leqslant T$ (phase II), the optimal controls are $u_1(t)=u_2(t)=1$.

(3) $T>T_B$ (case B2): Here the optimal pulse sequence has three distinct phases [see Fig. 3(a)]. There are two switching times τ_1 and $T-\tau_2$. Phases I and II are the same as above: For $0\leqslant t\leqslant\tau_1$ (phase I), $u_2(t)=1$ and $u_1(t)$ is increased gradually from a value $u_1(0)<1$ to $u_1(\tau_1)=1$. For time $\tau_1\leqslant t\leqslant T-\tau_2$ (phase II), the optimal controls are $u_1(t)=u_2(t)=1$. Finally, for $T-\tau_2\leqslant t\leqslant T$ (phase III), we have $u_1(t)=1$ and $u_2(t)$ is decreased from $u_2(T-\tau_2)=1$ to $u_2(T)<1$.

We now give physical explanation for the existence of these three cases. For small enough T, the major limitation for the transfer $r_1(0)\rightarrow r_2(T)$ is not the relaxation, but the limited available time. The optimal choice $u_1=u_2=1$ maximizes (absolute value) the off-diagonal elements $\pm u_1u_2$, which accomplish the transfer $r_1(t)\rightarrow r_2(t)$, as can be seen from the system equation (28). It also maximizes the diagonal elements, i.e., the relaxation rates of $r_1(t),r_2(t)$. But for small available time T, the gain that we get by maximizing the desired transfer at each moment t is more important than the (small) relaxation losses. As time T increases, the relaxation degrades more the performance and the choice $u_1=u_2=1$ ceases to be optimal. With $u_1<1$ or $u_2<1$ we may reduce the transfer rate of $r_1(t)\rightarrow r_2(t)$, but at the same time we decrease also the instantaneous relaxation rates $\xi_iu_i^2+\overline{\xi_i},i=1,2$. Since for large enough T the relaxation dominates, we conclude that by an appropriate choice of $u_1\leqslant 1$ or $u_2\leqslant 1$ we can get a better efficiency for the transfer $r_1(0)\rightarrow r_2(T)$. This appropriate choice corresponds to the cases B1 and B2. Note that for $k_1<k_2$, the system in case B2 spends more time in phase I ($u_1<1,u_2=1$) than in phase III ($u_1=1,u_2<1$), see Fig. 3(a). This happens because for $k_1<k_2$ and $u_1=u_2=u<1$, the relaxation rate $\xi_1u_1^2+\overline{\xi_1}$ is lower than the rate $\xi_2u_2^2+\overline{\xi_2}$ [note $\xi_1u_1^2+\overline{\xi_1}-\xi_2u_2^2-\overline{\xi_2}=(\xi_1-\xi_2)u^2+\overline{\xi_1}-\overline{\xi_2}<\xi_1-\xi_2+\overline{\xi_1}-\overline{\xi_2}=0$, since $\xi_1+\overline{\xi_1}=\xi_2+\overline{\xi_2}=k/J$]. Based on the above observation about the duration of phases I and III, we expect that as we increase T, from values where case A holds to values where case B2 is the optimal, there must be an intermediate range of values of T where the optimal pulse sequence has no phase III at all. This is the case B1.

The duration T_A above which the optimal pulse sequence is different than INEPT is $T_A=\cot^{-1}(2\xi_1)/\pi J$, for $\xi_1>\xi_2$. We can explain the dependence of this quantity on the parameters k,k_1. Note that $\xi_1=(k-k_1)/J$, so T_A is a decreasing function of k and an increasing function of k_1. For larger k (larger transverse relaxation) it is more costly to have the vectors $\boldsymbol{r}_1,\boldsymbol{r}_2$ parallel to the xy plane, i.e., it is more costly to have $u_1=u_2=1$ (see Fig. 1). This explains why T_A, which determines the range of values of T where the INEPT pulse sequence is optimal, is decreased. Now for larger k_1 (larger longitudinal relaxation) it is more costly to have the vector $\boldsymbol{r}_1$ parallel to the z axis, i.e., to have $u_1<1$. This explains why T_A, and with it the range of optimality of INEPT, is increased.

The switching time τ_1 for case B1 is calculated using the following equation:

$$T-\tau_1=\frac{1}{\pi J}\left(\frac{\pi}{2}-\varphi_1\right), \tag{30}$$

where

$$\varphi_1=\tan^{-1}\frac{2\xi_1}{1-\kappa_1(\tau_1)}$$

and

$$\kappa_1(t)=1+2\xi_1^2-2\xi_1\sqrt{1+\xi_1^2}\times\coth(\pi Jt\sqrt{1+\xi_1^2}+2\sinh^{-1}\xi_1).$$

The switching times for case B2 are calculated by solving the following system of equations:

$$T-\tau_1-\tau_2=\frac{\vartheta_2-\vartheta_1}{\pi J}, \tag{31}$$

$$T-\tau_1-\tau_2=\frac{\varphi_2-\varphi_1}{\pi J}, \tag{32}$$

where φ_1 as above and

$$\vartheta_1=\tan^{-1}\frac{2\xi_1\kappa_1(\tau_1)}{1-\kappa_1(\tau_1)},\quad \vartheta_2=\tan^{-1}\frac{1-\kappa_2(\tau_2)}{2\xi_2},$$

$$\varphi_2=\tan^{-1}\frac{1-\kappa_2(\tau_2)}{2\xi_2\kappa_2(\tau_2)}.$$

Function $\kappa_2(t)$ is given by a similar formula as $\kappa_1(t)$, with ξ_1 replaced by ξ_2. The relation of these angles to the optimal control problem is explained in Appendix A. The time T_B mentioned above can be found by solving Eqs. (31) and (32) for $\tau_2=0$, i.e., with unknowns T_B and τ_1. In other words, we find the time T_B for which the optimal pulse sequence develops the additional phase III by setting the duration of that phase equal to zero.

The results for $\xi_1<\xi_2$ ($k_1>k_2$) are analogous. The basic difference is for the case B1 (that with only one switching time). Here, we start in phase II ($u_1=u_2=1$) and at time $t=T-\tau_2$ we switch to case III, as it is shown in Fig. 2(b). The time τ_2 is calculated by

$$T-\tau_2=\frac{\vartheta_2}{\pi J}=\frac{1}{\pi J}\tan^{-1}\frac{1-\kappa_2(\tau_2)}{2\xi_2}. \tag{33}$$

For case B2 (that with the two switching times) we have three phases, as before, but now we spend more time in phase III than in phase I [see Fig. 3(b)]. The times τ_1, τ_2 are still calculated using Eqs. (31) and (32).

We describe also what happens for the symmetric case $\xi_1=\xi_2=\zeta$. In this case, the optimal pulse sequence spends equal time τ in phases I and III (see Fig. 4).

Note that when $\xi_1=\xi_2$ there is no intermediate case (B1, with only one switching time). Here, the optimal pulse sequence is either the INEPT or that with the three phases (and the two switching times). The time τ can be calculated by solving the equation

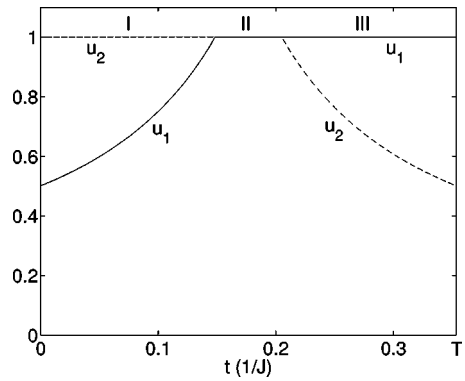

FIG. 4. Optimal pulse sequence for $k_1=k_2$. Observe the symmetry in the controls. Specifically, the relation $u_1(t)=u_2(T-t)$ holds here. For the values $k=J, k_1=k_2=0.20J$ that we use, the optimal duration is $T_{opt}\simeq 0.353J^{-1}$.

$$T-2\tau=\frac{1}{\pi J}\left[\tan^{-1}\frac{1-\kappa(\tau)}{2\zeta}-\tan^{-1}\frac{2\zeta\kappa(\tau)}{1-\kappa(\tau)}\right], \tag{34}$$

where $\kappa(\tau)$ is given by the formula for $\kappa_1(t)$, with ξ_1 replaced by ζ.

For each of the cases presented above, the maximum transfer efficiency $\eta_T=r_2(T)$ is calculated in Appendix B. The results are

(1) Case A (INEPT),

$$\eta_T=e^{-\pi kT}\sin(\pi JT). \tag{35}$$

(2) Case B1 (one switch),

$$\eta_T=e^{-\pi[k_1\tau_1+k(T-\tau_1)]}\sqrt{1-\xi_1\sin 2\varphi_1}, \tag{36}$$

for $k1<k2$ and

$$\eta_T=e^{-[k_2\tau_2+k(T-\tau_2)]}\sqrt{1-\xi_2\sin 2\vartheta_2}, \tag{37}$$

for $k1>k2$

(3) Case B2 (two switches),

$$\eta_T=\exp\{-\pi[k_1\tau_1+k(T-\tau_1-\tau_2)+k_2\tau_2]\}\frac{\sqrt{1-\xi_1\sin 2\varphi_1}\sqrt{1-\xi_2\sin 2\vartheta_2}}{\cos(\varphi_1-\vartheta_1)}. \tag{38}$$

In general, we can easily prove that the efficiency remains the same if the values of k_1 and k_2 are swapped. In Fig. 5 we plot the efficiency η_T as a function of T for various values of the parameters k,k_1,k_2.

We observe that for $k,k_1,k_2\neq 0$ there is an optimal time $T=T_{opt}$ for each choice of the parameters, while for $k_1=0$ or $k_2=0$ the maximum efficiency (maximum for T specified) increases with increasing T and approaches a limiting value as $T\to\infty$. The existence of this optimal duration T is a consequence of the fact that for $k_1,k_2\neq 0$ none of the operators $I_z, 2I_zS_z$ is protected against relaxation, while for $k_1=0$ or $k_2=0$ at least one of them is. We can explain the existence of this optimal T intuitively. For small T the available time for the application of the controls is not enough (we cannot

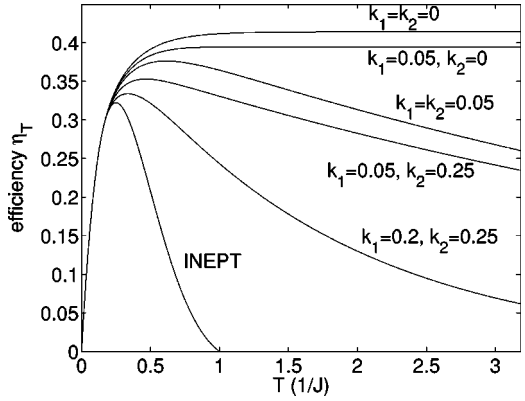

FIG. 5. Optimal transfer efficiency η_T as a function of the total transfer time T for $k=J$ and various values of k_1,k_2 (normalized with respect to J). Observe that for $k_1,k_2\neq 0$ there is an optimal transfer time T_{opt}.

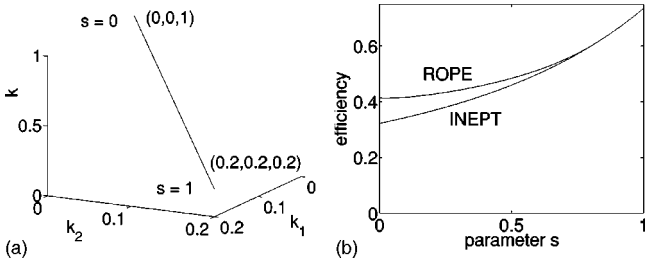

FIG. 6. (b) Maximum transfer efficiency η_T evaluated at T_{opt} for each point of the line in (k_1,k_2,k) space shown in (a). The line is parametrized by the parameter $0\leqslant s\leqslant 1$ and has been chosen such that the increase of s from 0 to 1 simulates the transition from slow molecular motion, where $k\gg k_1\simeq k_2$, to rapid molecular motion, where $k\simeq k_1\sim k_2$. Note the superiority of the relaxation optimized pulse element (ROPE) compared to the INEPT pulse sequence for the case $k\gg k_1\simeq k_2$.

"put" much control to the system) and thus the maximum efficiency that we get is small. For large T the phenomenon of relaxation dominates, since there is no operator protected against it, and the maximum efficiency that we achieve is poor. So, there must be an intermediate time T such that η_T becomes maximum. This time is T_{opt}. In Fig. 6(b) we plot the maximum efficiency, calculated at T_{opt} for each choice of the parameters, along a specific line in (k_1,k_2,k) space. This line is shown in Fig. 6(a) and has been chosen to simulate the transition from the slow molecular motion (slowly tumbling regime), where $k\gg k_1\simeq k_2$, to the rapid molecular motion, where $k\simeq k_1\sim k_2$.

For $0\leqslant t\leqslant \tau_1$ (phase I), the optimal control is given by

$$u_1(t)=\sqrt{\frac{\overline{\Lambda}_2^2[1+\cosh\phi_1(t)]}{2\overline{\Lambda}_1^2\sinh^2\phi_1\left(\frac{\tau_1}{2}\right)+\overline{\Lambda}_2^2\cosh\phi_1(\tau_1)-\overline{\Lambda}_2^2\cosh\phi_1(t)}}, \tag{39}$$

where $\phi_1(t)=2\pi Jt\sqrt{1+\xi_1^2}+2\sinh^{-1}\xi_1$ and

$$\overline{\Lambda}_1=\frac{\eta_T}{\sqrt{1+\kappa_1(\tau_1)\tan^2\varphi_1}},\quad \overline{\Lambda}_2=\frac{\eta_T}{\sqrt{\kappa_1(\tau_1)+\frac{1}{\tan^2\varphi_1}}}. \tag{40}$$

For $T-\tau_2\leqslant t\leqslant T$ (phase III), the optimal control is

$$u_2(t)=\sqrt{\frac{\overline{R}_1^2[1+\cosh\phi_2(T-t)]}{2\overline{R}_2^2\sinh^2\phi_2\left(\frac{\tau_2}{2}\right)+\overline{R}_1^2\cosh\phi_2(\tau_2)-\overline{R}_1^2\cosh\phi_2(T-t)}}, \tag{41}$$

where $\phi_2(t)=2\pi Jt\sqrt{1+\xi_2^2}+2\sinh^{-1}\xi_2$ and

$$\overline{R}_1=\frac{\eta_T}{\sqrt{\kappa_2(\tau_2)+\tan^2\vartheta_2}},\quad \overline{R}_2=\frac{\eta_T}{\sqrt{1+\frac{\kappa_2(\tau_2)}{\tan^2\vartheta_2}}}. \tag{42}$$

The corresponding rf amplitude for phase I is given by

$$\omega_y=\gamma_I B_y=2\pi J\frac{u_1}{\sqrt{1-u_1^2}}\tanh\left(\frac{\phi_1}{2}\right)\sqrt{1+\xi_1^2} \tag{43}$$

and for phase III by

$$\omega_x=\gamma_I B_x=2\pi J\frac{u_2^3}{\sqrt{1-u_2^2}}\tanh\left(\frac{\phi_2(T-t)}{2}\right)\sqrt{1+\xi_2^2}, \tag{44}$$

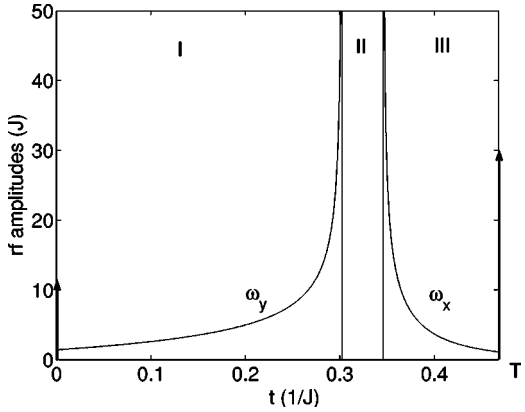

FIG. 7. The rf pulse sequence corresponding to the controls u_1, u_2 of Fig. 3(a). The pulse sequence starts with a hard 13.30° pulse around y axis, which establishes $u_1(0)=0.229$, followed by phase I as shown above. During phase II, no rf pulses are applied. Approaching phase II the rf amplitude becomes large for a very short time period. This can experimentally be very well approximated by a hard pulse of small flip angle. Following phase III as shown above, we apply a final hard 35.20° pulse around the x axis, which completes the transfer.

where γ_I is the gyromagnetic ratio of spin I. The details of these calculations are described in Appendix C. Note the asymmetry in the expressions for ω_x, ω_y, while the expressions for u_1, u_2 are symmetric. This asymmetry is a direct consequence of the phenomenon of relaxation. We refer to Fig. 1. Observe that the magnetic field B_y rotates the vector $\boldsymbol{r}_1$ clockwise, while the phenomenon of relaxation (dissipation of $\langle I_x \rangle$ with rate πk and of $\langle I_z \rangle$ with rate πk_1) rotates $\boldsymbol{r}_1$ counterclockwise, since $k > k_1$. On the other hand, both the magnetic field B_x and the phenomenon of relaxation rotate $\boldsymbol{r}_2$ counterclockwise, i.e., in the same sense. This difference between the two cases is the origin of the asymmetry in the expressions for ω_x, ω_y.

The optimal rf amplitudes for a specific choice of the parameters are shown in Fig. 7. The optimal transfer strategy from $I_z \rightarrow 2I_zS_z$ is then as follows. We start with an initial hard pulse that precedes phase I and rotates the vector $\boldsymbol{r}_1$ (Fig. 1), from the angle $\beta_1(0^-)=90°$ (parallel to z axis) to the initial angle $\beta_1(0^+)=\cos^{-1}u_1(0)$. During phase I ($0^+ \leqslant t \leqslant \tau_1$), we rotate $\boldsymbol{r}_1$ slowly towards the x axis using the field $B_y(t)$. During phase II ($\tau_1 \leqslant t \leqslant T-\tau_2$), no rf pulses are applied. We just let $\boldsymbol{r}_1$ evolve towards $\boldsymbol{r}_2$ on the xy plane. In phase III ($T-\tau_2 \leqslant t \leqslant T^-$), we rotate $\boldsymbol{r}_2$ slowly from the y axis towards the z axis using the field $B_x(t)$, up to the angle $\beta_2(T^-)=\cos^{-1}u_2(T)$. Following phase III, we apply a final hard pulse that rotates $\boldsymbol{r}_2$ from $\beta_2(T^-)$ to $\beta_2(T^+)=90°$, in order to complete the transfer to $2I_zS_z$. This optimal pulse sequence takes the place of INEPT. For the transfer $I_\alpha \rightarrow 2I_\beta S_\gamma$, we just need to include the appropriate initial and final hard 90° pulses.

Note that approaching phase II the rf amplitude becomes large for a very short time period. This can experimentally be very well approximated by a hard pulse of small flip angle.

Up to this point we have considered in detail the optimal way for the transfer $I_z \rightarrow 2I_zS_z$. The optimal transfer $I_z \rightarrow S_z$ is achieved by first doing the transfer $I_z \rightarrow 2I_zS_z$ optimally, followed by optimal transfer of $2I_zS_z \rightarrow S_z$. The optimal pulse sequence for the later transfer is analogous to the pulse sequence as discussed in the paper, with spin S playing the role of spin I and k_1, k_2 now representing the relaxation rates of longitudinal operators $2I_zS_z$ and S_z, respectively. Now k represents the transverse relaxation rates for operators $2I_zS_x, S_x$, etc.

V. CONCLUSION

In this manuscript, we examined the application of optimal control theory to a quantum-mechanical system in the presence of relaxation. The focus was on the study of an isolated pair of scalar coupled heteronuclear spins under dipole-dipole and chemical shift anisotropy relaxation. For this example, a new transfer scheme was found, which yields substantial gains in transfer efficiency, compared to the traditionally used INEPT pulse sequence. The methods presented here are by no means limited to the case of coupled two spins. They can be generalized for finding relaxation optimized pulse sequences for larger spin systems, as commonly encountered in backbone and side chain assignments in protein NMR spectroscopy. Furthermore, these methods are expected to find applications in the coherent control of other quantum-mechanical phenomena in the presence of dissipation and decoherence.

ACKNOWLEDGMENTS

N.K. acknowledges Darpa Grant No. 496020-01-1-0556, NSF Grant No. 0218411, and NSF Grant No. 0133673 for the support. S.J.G. acknowledges funding from Fonds der Chemischen Industrie, and by the Deutsche Forschungsgemeinschaft (Grant Nos. Gl 203/4-2 and Lu 835/1).

APPENDIX A: SOLUTION OF THE OPTIMAL CONTROL PROBLEM

The solution of the optimal control problem depends on the relative magnitude of the parameters ξ_1, ξ_2. In the following, we solve the problem for the nonsymmetric case $\xi_1 > \xi_2$, i.e., $k_1 < k_2$. The results for the case $\xi_1 < \xi_2$ ($k_1 > k_2$) are analogous. At the end of this section we describe also what happens for the symmetric case $\xi_1 = \xi_2$.

To find the optimal controls $(u_1^*(t), u_2^*(t))$ in Eq. (28), we use the principle of dynamic programming [14] and solve for the maximum achievable value of r_2 for all initial points (r_1, r_2). Starting from (r_1, r_2), we denote the maximum achievable value of r_2 by $V(r_1, r_2, t)$, also called the optimal return function for the point (r_1, r_2) at time t. Note here that for the finite time problem (T finite), the optimal return function has explicit dependence on time [14]. If we start at (r_1, r_2), then by making a choice of controls in Eq. (28) and letting the dynamical system evolve, after small time δt we can make a transition to all points $(\tilde{r}_1, \tilde{r}_2)$ which are related to (r_1, r_2) by

$$\begin{bmatrix}\tilde{r}_1\\ \tilde{r}_2\end{bmatrix}=\begin{bmatrix}r_1\\ r_2\end{bmatrix}+\delta t\begin{bmatrix}-\xi_1u_1^2-\overline{\xi_1} & -u_1u_2\\ u_1u_2 & -\xi_2u_2^2-\overline{\xi_2}\end{bmatrix}\begin{bmatrix}r_1\\ r_2\end{bmatrix}. \tag{A1}$$

From all points $(\tilde{r}_1,\tilde{r}_2)$ that can be reached by appropriate choice of (u_1,u_2) in small time δt, we should choose to go to that $(\tilde{r}_1,\tilde{r}_2)$ for which $V(\tilde{r}_1,\tilde{r}_2,t+\delta t)$ is the largest. But now note by definition of V that $V(r_1,r_2,t)=\max_{\tilde{r}_1,\tilde{r}_2}V(\tilde{r}_1,\tilde{r}_2,t+\delta t)$. This can be rewritten as

$$V(r_1,r_2,t)=\max_{u_1,u_2}V\{r_1+\delta t[(-\xi_1u_1^2-\overline{\xi_1})r_1-u_1u_2r_2],$$

$$r_2+\delta t[(-\xi_2u_2^2-\overline{\xi_2})r_2+u_1u_2r_1],t+\delta t\}, \tag{A2}$$

for infinitesimal δt. The right-hand side of the above expression can be expanded (Taylor series expansion) in powers of δt and retaining only the terms linear in δt (for δt approaching zero), we obtain the well-known Hamilton Jacobi Bellman equation

$$\frac{\partial V}{\partial t}+\max_{u_1,u_2}H(u_1,u_2)=0, \tag{A3}$$

where

$$H(u_1,u_2)=\begin{bmatrix}\frac{\partial V}{\partial r_1} & \frac{\partial V}{\partial r_2}\end{bmatrix}\begin{bmatrix}-\xi_1u_1^2-\overline{\xi_1} & -u_1u_2\\ u_1u_2 & -\xi_2u_2^2-\overline{\xi_2}\end{bmatrix}\begin{bmatrix}r_1\\ r_2\end{bmatrix} \tag{A4}$$

is the Hamiltonian for the optimal control problem. Let

$$\lambda_1=\frac{\partial V}{\partial r_1},\quad \lambda_2=\frac{\partial V}{\partial r_2}. \tag{A5}$$

If, additionally, we set

$$a=\frac{\lambda_2}{\lambda_1},\quad b=\frac{r_2}{r_1}, \tag{A6}$$

then the Hamiltonian can be expressed as

$$H(u_1,u_2)=-\lambda_1r_1[\xi_1u_1^2-(a-b)u_1u_2+ab\xi_2u_2^2+\overline{\xi_1}+ab\overline{\xi_2}]. \tag{A7}$$

The optimal return function is a nondecreasing function of r_1,r_2 [starting from a larger $r_1(0)$ or $r_2(0)$ you can achieve a larger $r_2(T)$] so $\lambda_1,\lambda_2,a\geq 0$. Since $\lambda_1,r_1\geq 0$, in order to maximize H in the square $0\leq u_1,u_2\leq 1$ it is equivalent to minimizing the function

$$F(u_1,u_2)=\xi_1u_1^2-(a-b)u_1u_2+ab\xi_2u_2^2+\overline{\xi_1}+ab\overline{\xi_2} \tag{A8}$$

or the quadratic form

$$Q(u_1,u_2)=\xi_1u_1^2-(a-b)u_1u_2+ab\xi_2u_2^2, \tag{A9}$$

which is the part of $F(u_1,u_2)$ that contains explicitly the controls u_1,u_2. Note that $a,b,\xi_1,\xi_2,u_1,u_2\geq 0$. If $(a-b)\leq 0$ then the solution to the minimization of $Q(u_1,u_2)$ is the trivial one $u_1=u_2=0$. Therefore $(a-b)>0$. Now suppose that $(a-b)^2\leq 4\xi_1\xi_2ab$, i.e., $(a-b)^2/4\xi_1\xi_2=ab-\epsilon$ for $\epsilon\geq 0$. Then

$$Q=\left[\frac{(a-b)}{2\sqrt{\xi_1}}u_2-\xi_1u_1\right]^2+\epsilon\xi_2u_2^2 \tag{A10}$$

and the solution to the minimization of Q is again the trivial one $u_1=u_2=0$. Therefore the acceptable case is $(a-b)^2>4\xi_1\xi_2ab$. Using the conditions

$$a-b>0,\ (a-b)^2>4\xi_1\xi_2ab, \tag{A11}$$

that we just derived, we minimize Q in the square $0\leq u_1,u_2\leq 1$. We find three separate cases (actually, there is one more case but, since it is not important for the rest of the problem, we do not present it).

(1) Case I: If $a-b<2\xi_1$ and $(a-b)/ab\geq 2\xi_2$, then the minimum of Q (maximum of H) is obtained for $u_2=1$ and $u_1=(a-b)/2\xi_1$.

(2) Case II: If $a-b\geq 2\xi_1$ and $(a-b)/ab\geq 2\xi_2$, then the minimum of Q is obtained for $u_1=1$ and $u_2=1$.

(3) Case III: If $a-b\geq 2\xi_1$ and $(a-b)/ab<2\xi_2$, then the minimum of Q is obtained for $u_1=1$ and $u_2=(a-b)/2\xi_2ab$.

It is a standard result [14] that, along the optimal trajectory $(r_1^*(t),r_2^*(t))$, the adjoint variables

$$(\lambda_1(t),\lambda_2(t))=\left(\frac{\partial V}{\partial r_1},\frac{\partial V}{\partial r_2}\right)\Bigg|_{(r_1^*(t),r_2^*(t))}$$

satisfy the equations $\dot{\lambda}_1=-\partial H/\partial r_1$ and $\dot{\lambda}_2=-\partial H/\partial r_2$, i.e.,

$$\frac{d}{dt}\begin{bmatrix}\lambda_1\\ \lambda_2\end{bmatrix}=\begin{bmatrix}\xi_1u_1^2+\overline{\xi_1} & -u_1u_2\\ u_1u_2 & \xi_2u_2^2+\overline{\xi_2}\end{bmatrix}\begin{bmatrix}\lambda_1\\ \lambda_2\end{bmatrix}, \tag{A12}$$

with the terminal conditions

$$\lambda_1(T)=0,\quad \lambda_2(T)=1. \tag{A13}$$

For the optimal trajectory starting at $(r_1,r_2)=(1,0)$ it is $b(0)=0$, so depending on $a(0)$ we have the following cases.

Case A. If $a(0)\geq 2\xi_1$ (first condition) then we start in case II discussed above. We stay there for the whole interval T if (note that $a-b$ is increasing) $[a(T)-b(T)]/a(T)b(T)\geq 2\xi_2$ (second condition). In case II, $u_1=u_2=1$ and using Eqs. (28) and (A12) we can find $a(T),b(T)$ in terms of $a(0)$ and $b(0)=0$. It is $a(T)=[a(0)+\tan T]/[1-a(0)\tan T]$, $b(T)=\tan T$ so

$$\frac{a(T)-b(T)}{a(T)b(T)}=\frac{a(0)(1+\tan^2T)}{\tan T[a(0)+\tan T]}. \tag{A14}$$

Now note that $a(T)=\lambda_2(T)/\lambda_1(T)=\infty$ since $\lambda_1(T)=0$, so must be $a(0)=1/\tan T$ if we spend the whole interval in case II. For $\tan T \leqslant 1/2\xi_1$ it is $a(0)\geqslant 2\xi_1$, so we are consistent with the first condition, and $[a(T)-b(T)]/[a(T)b(T)] = 1/\tan T \geqslant 2\xi_1 > 2\xi_2$, so we are also consistent with the second condition. The conclusion is that for $\tan T \leqslant 1/2\xi_1$ we start in case II and stay there for the whole time interval T. This corresponds to the INEPT pulse sequence.

Case B. If $a(0)<2\xi_1$ we start in case I. In this case it is $u_2=1$, $u_1=(a-b)/2\xi_1$ and the equation for the state variables becomes

$$\frac{d}{dt}\begin{bmatrix} r_1 \\ r_2 \end{bmatrix}=\begin{bmatrix} -\xi_1 u_1^2-\overline{\xi_1} & -u_1 \\ u_1 & -\xi_2-\overline{\xi_2} \end{bmatrix}\begin{bmatrix} r_1 \\ r_2 \end{bmatrix}. \tag{A15}$$

But $\xi_1+\overline{\xi_1}=\xi_2+\overline{\xi_2}=k/J$ so the above equation is the same as

$$\frac{d}{dt}\begin{bmatrix} r_1 \\ r_2 \end{bmatrix}=\begin{bmatrix} -\xi_1 u_1^2-\overline{\xi_1} & -u_1 \\ u_1 & -\xi_1-\overline{\xi_1} \end{bmatrix}\begin{bmatrix} r_1 \\ r_2 \end{bmatrix}. \tag{A16}$$

If we make the transformation $\overline{r_i}=e^{\overline{\xi_1}t}r_i$ we get

$$\frac{d}{dt}\begin{bmatrix} \overline{r_1} \\ \overline{r_2} \end{bmatrix}=\begin{bmatrix} -\xi_1 u_1^2 & -u_1 \\ u_1 & -\xi_1 \end{bmatrix}\begin{bmatrix} \overline{r_1} \\ \overline{r_2} \end{bmatrix}. \tag{A17}$$

Analogously, for the adjoint variables we find the equation

$$\frac{d}{dt}\begin{bmatrix} \overline{\lambda_1} \\ \overline{\lambda_2} \end{bmatrix}=\begin{bmatrix} \xi_1 u_1^2 & -u_1 \\ u_1 & \xi_1 \end{bmatrix}\begin{bmatrix} \overline{\lambda_1} \\ \overline{\lambda_2} \end{bmatrix}, \tag{A18}$$

where $\overline{\lambda_i}=e^{-\overline{\xi_1}t}\lambda_i$. Now observe that $\overline{b}/\overline{a}=\overline{r_2}\overline{\lambda_1}/\overline{r_1}\overline{\lambda_2} = b/a$. If we set $\overline{b}/\overline{a}=b/a=\kappa_1(t)$ then $\kappa_1(0)=0$ and $\kappa_1(t)$ satisfies the differential equation

$$\frac{d\kappa_1}{dt}=\frac{(\kappa_1-1)^2}{2\xi_1}-2\xi_1\kappa_1. \tag{A19}$$

This can be proved using Eqs. (A17) and (A18). So $b/a(t)$ satisfies Eq. (A19) for case I. After time τ_1, $(a-b)/2\xi_1$ becomes equal to 1 and the system switches to case II. Using $[a(\tau_1)-b(\tau_1)]/2\xi_1=1$ and that $(b/a)(\tau_1)=\kappa_1(\tau_1)$ we find

$$a(\tau_1)=\frac{\lambda_2(\tau_1)}{\lambda_1(\tau_1)}=\frac{2\xi_1}{1-\kappa_1(\tau_1)}\equiv\tan\varphi_1, \tag{A20}$$

$$b(\tau_1)=\frac{r_2(\tau_1)}{r_1(\tau_1)}=\frac{2\xi_1\kappa_1(\tau_1)}{1-\kappa_1(\tau_1)}\equiv\tan\vartheta_1 \quad . \tag{A21}$$

As time goes by $(a-b)/ab$ decreases. If this fraction does not reach the value $2\xi_2$ in the remaining time interval $[\tau_1,T]$ then the system remains in case II and we call this case B1. Else, the system switches to case III and we call this case B2. We examine first the full scenario (case B2). Suppose that $(a-b)/ab=2\xi_2$ at time $T-\tau_2$. This is the switching time from case II to case III. If we work as before we find that in case III, $(b/a)(t)=\kappa_2(T-t)$ where $\kappa_2(t)$ satisfies the differential equation

$$\frac{d\kappa_2}{dt}=\frac{(\kappa_2-1)^2}{2\xi_2}-2\xi_2\kappa_2, \quad \kappa_2(0)=0. \tag{A22}$$

For $t=T-\tau_2$ it is $b(T-\tau_2)/a(T-\tau_2)=\kappa_2(\tau_2)$ and $[a(T-\tau_2)-b(T-\tau_2)]/[a(T-\tau_2)b(T-\tau_2)]=2\xi_2$. Using these we find

$$a(T-\tau_2)=\frac{\lambda_2(T-\tau_2)}{\lambda_1(T-\tau_2)}=\frac{1-\kappa_2(\tau_2)}{2\xi_2\kappa_2(\tau_2)}\equiv\tan\varphi_2, \tag{A23}$$

$$b(T-\tau_2)=\frac{r_2(T-\tau_2)}{r_1(T-\tau_2)}=\frac{1-\kappa_2(\tau_2)}{2\xi_2}\equiv\tan\vartheta_2. \tag{A24}$$

In order to find the switching times $\tau_1, T-\tau_2$ we have to connect Eqs. (A20) and (A21) with Eqs. (A23) and (A24). We can do so by examining the evolution of the system while it is in case II, i.e., in the time interval $[\tau_1, T-\tau_2]$. In case II it is $u_1=u_2=1$ so the system equation (28) becomes

$$\frac{d}{dt}\begin{bmatrix} r_1 \\ r_2 \end{bmatrix}=\begin{bmatrix} -\xi & -1 \\ 1 & -\xi \end{bmatrix}\begin{bmatrix} r_1 \\ r_2 \end{bmatrix}, \tag{A25}$$

where $\xi=\xi_1+\overline{\xi_1}=\xi_2+\overline{\xi_2}$. This is the same as the system equation for a damped harmonic oscillator with angular frequency $\omega=1$. From $t=\tau_1$ to $t=T-\tau_2$ the vector (r_1,r_2) is rotated through the angle

$$\vartheta_2-\vartheta_1=T-\tau_1-\tau_2=\tan^{-1}\frac{1-\kappa_2(\tau_2)}{2\xi_2}-\tan^{-1}\frac{2\xi_1\kappa_1(\tau_1)}{1-\kappa_1(\tau_1)}. \tag{A26}$$

The evolution equation for the adjoint variables in case II is

$$\frac{d}{dt}\begin{bmatrix} \lambda_1 \\ \lambda_2 \end{bmatrix}=\begin{bmatrix} \xi & -1 \\ 1 & \xi \end{bmatrix}\begin{bmatrix} \lambda_1 \\ \lambda_2 \end{bmatrix}. \tag{A27}$$

The vector (λ_1,λ_2) is rotated through the angle

$$\varphi_2-\varphi_1=T-\tau_1-\tau_2=\tan^{-1}\frac{1-\kappa_2(\tau_2)}{2\xi_2\kappa_2(\tau_2)}-\tan^{-1}\frac{2\xi_1}{1-\kappa_1(\tau_1)}. \tag{A28}$$

Equations (A26) and (A28) constitute a system of two equations for the two unknowns τ_1,τ_2 which can be solved numerically. For the case B1 there is only one switching time (τ_1) and working analogously we can easily find that it satisfies the equation

$$T-\tau_1=\varphi_2-\varphi_1=\frac{\pi}{2}-\tan^{-1}\frac{2\xi_1}{1-\kappa_1(\tau_1)}. \tag{A29}$$

As we showed above, case B happens when the duration of the experiment satisfies $T>T_A=\tan^{-1}(1/2\xi_1)$. The question is when we are in case B1 and when in case B2. Intuitively, we expect that up to some duration T_B we have to apply the controls of case B1 and for $T>T_B$, where the phenomenon

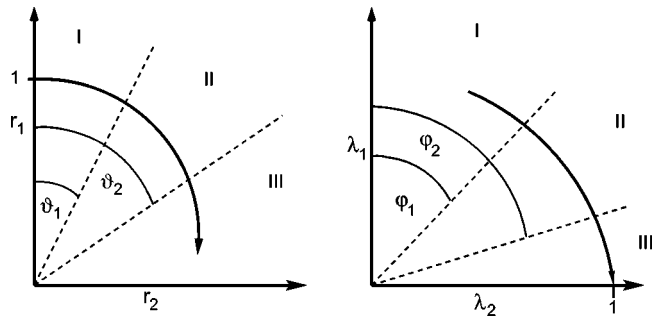

FIG. 8. Figure depicts the angles ϑ_1, ϑ_2 and φ_1, φ_2, the optimal trajectory $(r_1(t), r_2(t))$ and the trajectory for the adjoint variables $(\lambda_1(t), \lambda_2(t))$.

of relaxation degrades more the performance, we need to apply the more fancy controls of case B2. T_B can be obtained from Eqs. (A26) and (A28) by substituting $\tau_2 = 0$. So, we have a system of two equations with unknowns the duration T_B and the switching time τ_1 and thus we can find T_B. For $T < T_B$ the system of Eqs. (A26) and (A28) gives $\tau_2 < 0$, while for $T > T_B$ gives $\tau_2 > 0$. Note that all the times that appear in this section are normalized according to $t_{new} = \pi J t_{old}$.

The results for $\xi_1 < \xi_2$ $(k_1 > k_2)$ are analogous. The basic difference is for the case B1 (that with only one switching time). Here, we start in phase II $(u_1 = u_2 = 1)$ and at time $t = T - \tau_2$ we switch to case III, as it is shown in Fig. 2(b). The time τ_2 is calculated by

$$T - \tau_2 = \vartheta_2 - \vartheta_1 = \tan^{-1} \frac{1 - \kappa_2(\tau_2)}{2\xi_2}. \tag{A30}$$

For case B2 (that with the two switching times) we have three phases, as before, but now we spend more time in phase III than in phase I [see Fig. 3(b)]. The times τ_1, τ_2 are still calculated using Eqs. (A26) and (A28).

Figure 8 depicts the angles ϑ_1, ϑ_2 and φ_1, φ_2, the optimal trajectory $(r_1(t), r_2(t))$ and the trajectory for the adjoint variables $(\lambda_1(t), \lambda_2(t))$.

Finally, we examine what happens for $\xi_1 = \xi_2 \equiv \zeta$. In this case it is $\kappa_1(t) = \kappa_2(t) \equiv \kappa(t)$, and Eqs. (A26) and (A28) take the form

$$T - \tau_1 - \tau_2 = \tan^{-1} \frac{1 - \kappa(\tau_2)}{2\zeta} - \tan^{-1} \frac{2\zeta\kappa(\tau_1)}{1 - \kappa(\tau_1)}, \tag{A31}$$

$$T - \tau_1 - \tau_2 = \tan^{-1} \frac{1 - \kappa(\tau_2)}{2\zeta\kappa(\tau_2)} - \tan^{-1} \frac{2\zeta}{1 - \kappa(\tau_1)}. \tag{A32}$$

If we set

$$f(\tau_1, \tau_2) = \tan^{-1} \frac{1 - \kappa(\tau_2)}{2\zeta} - \tan^{-1} \frac{2\zeta\kappa(\tau_1)}{1 - \kappa(\tau_1)}, \tag{A33}$$

it is not hard to see that

$$f(\tau_2, \tau_1) = \tan^{-1} \frac{1 - \kappa(\tau_2)}{2\zeta\kappa(\tau_2)} - \tan^{-1} \frac{2\zeta}{1 - \kappa(\tau_1)}, \tag{A34}$$

thus we end up with the system

$$T - \tau_1 - \tau_2 = f(\tau_1, \tau_2), \tag{A35}$$

$$T - \tau_1 - \tau_2 = f(\tau_2, \tau_1). \tag{A36}$$

These equations imply

$$f(\tau_1, \tau_2) = f(\tau_2, \tau_1). \tag{A37}$$

This gives

$$\tau_1 = \tau_2 \equiv \tau, \tag{A38}$$

so for the symmetric case $\xi_1 = \xi_2$ the optimal pulse sequence spends equal time τ in phases I and III (see Fig. 4). Note that for $\xi_1 = \xi_2$ there is no intermediate case (B1, with only one switching time). Here, the optimal pulse sequence is either the INEPT or that with the three phases (and the two switching times). The time τ can be calculated by using either of Eqs. (A31) and (A32) with $\tau_1 = \tau_2 = \tau$.

APPENDIX B: CALCULATION OF THE MAXIMUM TRANSFER EFFICIENCY

Here we derive the value of $\eta_T = r_2(T)$ for each of the cases presented in Appendix A.

Case A (INEPT). For $u_1 = u_2 = 1$ the system equation is Eq. (A25). With initial conditions $r_1(0) = 1, r_2(0) = 0$ we find

$$\eta_T = r_2(T) = e^{-\xi T} \sin T. \tag{B1}$$

Case B2. Using Eqs. (28) and (A12) we can show that

$$V(t) = \lambda_1(t) r_1(t) + \lambda_2(t) r_2(t), \quad 0 \leq t \leq T \tag{B2}$$

is a constant along the system trajectories and equals the optimal return function $V(t) = \lambda_1(0) = r_2(T)$. Analogously we can show that

$$V_1(t) = e^{-\bar{\xi}_1 t} \sqrt{\lambda_1^2(t) + \kappa_1(t)\lambda_2^2(t)}, \quad 0 \leq t \leq \tau_1 \tag{B3}$$

and

$$V_2(t) = e^{-\bar{\xi}_2 (T-t)} \sqrt{r_2^2(t) + \kappa_2(T-t) r_1^2(t)}, \tag{B4}$$

$T - \tau_2 \leq t \leq T$, are constants along the system trajectories with $V_1(t) = \lambda_1(0), V_2(t) = r_2(T)$. So they are also equal to the optimal return function. Define

$$R(t) = \sqrt{r_1^2(t) + r_2^2(t)}, \quad \Lambda(t) = \sqrt{\lambda_1^2(t) + \lambda_2^2(t)}. \tag{B5}$$

Since $r_2/r_1 = \tan\vartheta$ and $\lambda_2/\lambda_1 = \tan\varphi$ it is also $r_2 = R \sin\vartheta, r_1 = R\cos\vartheta$ and $\lambda_2 = \Lambda \sin\varphi, \lambda_1 = \Lambda\cos\varphi$. Using these relations and Eq. (B3) we find

$$V_1(\tau_1) = e^{-\bar{\xi}_1 \tau_1} \Lambda_1 \sqrt{1 - \xi_1 \sin 2\varphi_1}, \tag{B6}$$

where $\Lambda_1=\Lambda_1(\tau_1)$. Using Eq. (B2) we find

$$V(\tau_1)=\Lambda_1 R_1\cos(\varphi_1-\vartheta_1), \tag{B7}$$

where $R_1=R(\tau_1)$. Since $V(\tau_1)=V_1(\tau_1)$ from Eqs. (B6) and (B7) we easily deduce that

$$R_1=e^{-\bar{\xi}_1\tau_1}\frac{\sqrt{1-\xi_1\sin 2\varphi_1}}{\cos(\varphi_1-\vartheta_1)}. \tag{B8}$$

From Eq. (B4) we find

$$V_2(T-\tau_2)=e^{-\bar{\xi}_2\tau_2}R_2\sqrt{1-\xi_2\sin 2\vartheta_2}. \tag{B9}$$

But $R_2=R_1e^{-\xi(T-\tau_1-\tau_2)}$ (case II, damped harmonic oscillator). Using the above relations we find finally

$$\eta_T=\exp\{-[\bar{\xi}_1\tau_1+\xi(T-\tau_1-\tau_2)+\bar{\xi}_2\tau_2]\}\frac{\sqrt{1-\xi_1\sin 2\varphi_1}\sqrt{1-\xi_2\sin 2\vartheta_2}}{\cos(\varphi_1-\vartheta_1)}. \tag{B10}$$

Case B1. Following a procedure analogous to the above we can find that the maximum transfer efficiency in this case is given by

$$\eta_T=e^{-[\bar{\xi}_1\tau_1+\xi(T-\tau_1)]}\sqrt{1-\xi_1\sin 2\varphi_1}. \tag{B11}$$

This is the result for $k_1<k_2$. For $k_1>k_2$ the result is analogous,

$$\eta_T=e^{-[k_2\tau_2+k(T-\tau_2)]}\sqrt{1-\xi_2\sin 2\vartheta_2}. \tag{B12}$$

APPENDIX C: CALCULATION OF THE OPTIMAL CONTROLS AND OF THE CORRESPONDING rf FIELD

Case I ($0\leqslant t\leqslant\tau_1$). In this case $u_2=1$ and

$$u_1=\frac{a-b}{2\xi_1}=\frac{1}{2\xi_1}\frac{\lambda_2(t)}{\lambda_1(t)}[1-\kappa_1(t)].$$

The function $\kappa_1(t)$ is the solution of Eq. (A19) with initial condition $\kappa_1(0)=0$. We can easily find that $\kappa_1(t)=1+2\xi_1^2-2\xi_1\sqrt{1+\xi_1^2}\coth\bar{\phi}_1(t)$, where $\bar{\phi}_1(t)=t\sqrt{1+\xi_1^2}+2\sinh^{-1}\xi_1$ for t normalized or $\bar{\phi}_1(t)=\pi Jt\sqrt{1+\xi_1^2}+2\sinh^{-1}\xi_1$ for t not normalized. We still need to calculate $\lambda_1(t),\lambda_2(t)$. Using Eq. (A12) for the adjoint variables, we can see that $\lambda_2(t)$ satisfies the equation

$$\dot{\lambda}_2(t)=[\bar{\xi}_1+\sqrt{1+\xi_1^2}\coth\bar{\phi}_1(t)]\lambda_2 \tag{C1}$$

or

$$\dot{\bar{\lambda}}_2(t)=\sqrt{1+\xi_1^2}\coth\bar{\phi}_1(t)\bar{\lambda}_2, \tag{C2}$$

where as usual $\bar{\lambda}_2=e^{-\bar{\xi}_1 t}\lambda_2$. We can solve Eq. (C2) in the interval $0\leqslant t\leqslant\tau_1$ with final condition $\bar{\lambda}_2(\tau_1)=\bar{\Lambda}_2$ [we calculate $\bar{\Lambda}_2$ and $\bar{\Lambda}_1=\bar{\lambda}_1(\tau_1)$ later]. The solution is

$$\lambda_2(t)=e^{\bar{\xi}_1 t}\bar{\lambda}_2(t)=e^{\bar{\xi}_1 t}\bar{\Lambda}_2\frac{\sinh\bar{\phi}_1(t)}{\sinh\bar{\phi}_1(\tau_1)}. \tag{C3}$$

Now using the expression $\eta_T=e^{-\bar{\xi}_1 t}\sqrt{\lambda_1^2(t)+\kappa_1(t)\lambda_2^2(t)}$ for the optimal return function we have

$$\lambda_1(t)=\sqrt{e^{2\bar{\xi}_1 t}\eta_T^2-\kappa_1(t)\lambda_2^2(t)}. \tag{C4}$$

Using again the expression for η_T but with $t=\tau_1$ we find

$$\eta_T=e^{-\bar{\xi}_1\tau_1}\sqrt{\Lambda_1^2+\kappa_1(\tau_1)\Lambda_2^2}=\sqrt{\bar{\Lambda}_1^2+\kappa_1(\tau_1)\bar{\Lambda}_2^2}, \tag{C5}$$

where $\Lambda_1=\lambda_1(\tau_1)$, $\Lambda_2=\lambda_2(\tau_1)$ and $\bar{\Lambda}_1,\bar{\Lambda}_2$ as above. Combining Eqs. (C3)–(C5) we get

$$\lambda_1(t)=e^{\bar{\xi}_1 t}\sqrt{\bar{\Lambda}_1^2+\kappa_1(\tau_1)\bar{\Lambda}_2^2-\kappa_1(t)\bar{\Lambda}_2^2\frac{\sinh^2\bar{\phi}_1(t)}{\sinh^2\bar{\phi}_1(\tau_1)}}. \tag{C6}$$

Using Eqs. (C3) and (C6) we find

$$u_1(t)=\sqrt{\frac{\bar{\Lambda}_2^2[1+\cosh\phi_1(t)]}{2\bar{\Lambda}_1^2\sinh^2\phi_1\left(\frac{\tau_1}{2}\right)+\bar{\Lambda}_2^2\cosh\phi_1(\tau_1)-\bar{\Lambda}_2^2\cosh\phi_1(t)}}, \tag{C7}$$

where $\phi_1(t)=2\pi Jt\sqrt{1+\xi_1^2}+2\sinh^{-1}(\xi_1)$. In order to find $\bar{\Lambda}_1,\bar{\Lambda}_2$ we use Eq. (C5) and that $\bar{\Lambda}_2/\bar{\Lambda}_1=\Lambda_2/\Lambda_1=\tan\varphi_1$. We get

$$\bar{\Lambda}_1=\frac{\eta_T}{\sqrt{1+\kappa_1(\tau_1)\tan^2\varphi_1}},\quad \bar{\Lambda}_2=\frac{\eta_T}{\sqrt{\kappa_1(\tau_1)+\frac{1}{\tan^2\varphi_1}}}, \tag{C8}$$

where $\tan\varphi_1$ is given by Eq. (A20).

Case II ($\tau_1\leqslant t\leqslant\tau_2$). In this case, $u_1(t)=u_2(t)=1$.

Case III ($\tau_2\leqslant t\leqslant T$). In this case, $u_1=1$ and

$$u_2=\frac{a-b}{2\xi_2 ab}=\frac{1}{2\xi_2}\frac{r_1(t)}{r_2(t)}[1-\kappa_2(T-t)].$$

Following a procedure analogous to that for case I we finally find

$$u_2(t)=\sqrt{\frac{\overline{R}_1^2[1+\cosh\phi_2(T-t)]}{2\overline{R}_2^2\sinh^2\phi_2\left(\frac{\tau_2}{2}\right)+\overline{R}_1^2\cosh\phi_2(\tau_2)-\overline{R}_1^2\cosh\phi_2(T-t)}}, \tag{C9}$$

where

$$\phi_2(t)=2\pi Jt\sqrt{1+\xi_2^2}+2\sinh^{-1}\xi_2, \tag{C10}$$

$$\overline{R}_1=\frac{\eta_T}{\sqrt{\kappa_2(\tau_2)+\tan^2\vartheta_2}},\quad \overline{R}_2=\frac{\eta_T}{\sqrt{1+\frac{\kappa_2(\tau_2)}{\tan^2\vartheta_2}}} \tag{C11}$$

and $\tan\vartheta_2$ is given by Eq. (A24). We finally calculate the rf field that produces the optimal controls u_1,u_2. The infinitesimal change in angle β_1 (see Fig. 1) is given by

$$\delta\beta_1=\delta\overline{\beta}_1-\omega_y\delta t, \tag{C12}$$

where $\delta\overline{\beta}_1$ is the infinitesimal change when the magnetic field is zero, i.e., when the system evolves only under Eqs. (28), and $\omega_y=\gamma_I B_y$. We see that

$$\omega_y=\dot{\overline{\beta}}_1-\dot{\beta}_1. \tag{C13}$$

But $u_1=\cos\beta_1$, so

$$\dot{\beta}_1=-\frac{\dot{u}_1}{\sqrt{1-u_1^2}}. \tag{C14}$$

Using Eq. (C7) for u_1 we find, after some lengthy calculation, that

$$\dot{\beta}_1=-\pi J\frac{u_1(1+u_1^2)}{\sqrt{1-u_1^2}}\tanh\left(\frac{\phi_1}{2}\right)\sqrt{1+\xi_1^2}. \tag{C15}$$

When the magnetic field is zero it is $\beta_1=\overline{\beta}_1$ so $\tan\overline{\beta}_1=\langle I_z\rangle/\langle I_x\rangle$ and

$$\dot{\overline{\beta}}_1=\cos^2\beta_1\frac{d}{dt}\left(\frac{\langle I_z\rangle}{\langle I_x\rangle}\right)=u_1^2\frac{d}{dt}\left(\frac{\langle I_z\rangle}{\langle I_x\rangle}\right). \tag{C16}$$

We can find the time derivative above using the equations for the time derivatives of the ensemble averages presented in Sec. II. Doing so, we end up with the formula

$$\dot{\overline{\beta}}_1=\pi Ju_1\sqrt{1-u_1^2}\left(\xi_1+\frac{r_2}{r_1u_1}\right). \tag{C17}$$

But

$$\frac{r_2}{r_1}=b=u_1\frac{2\xi_1\kappa_1(t)}{1-\kappa_1(t)}$$

with $\kappa_1(t)$ given above. After some calculations we finally find

$$\dot{\overline{\beta}}_1=\pi Ju_1\sqrt{1-u_1^2}\tanh\left(\frac{\phi_1}{2}\right)\sqrt{1+\xi_1^2}. \tag{C18}$$

Combining Eqs. (C13), (C15), and (C18) we find that

$$\omega_y=\gamma_I B_y=2\pi J\frac{u_1}{\sqrt{1-u_1^2}}\tanh\left(\frac{\phi_1}{2}\right)\sqrt{1+\xi_1^2}. \tag{C19}$$

Working analogously we find

$$\omega_x=\gamma_I B_x=2\pi J\frac{u_2^3}{\sqrt{1-u_2^2}}\tanh\left(\frac{\phi_2(T-t)}{2}\right)\sqrt{1+\xi_2^2}.$$

The asymmetry in the expressions for ω_x,ω_y is a direct consequence of the phenomenon of relaxation and it is explained in Sec. IV.

[1] R.R. Ernst, G. Bodenhausen, and A. Wokaun, *Principles of Nuclear Magnetic Resonance in One and Two Dimensions* (Clarendon Press, Oxford, 1987).

[2] N. Khaneja, T. Reiss, B. Luy, and S.J. Glaser, J. Magn. Reson. **162**, 311 (2003).

[3] N. Khaneja, B. Luy, and S.J. Glaser, Proc. Natl. Acad. Sci. U.S.A. **100**, 13162 (2003).

[4] G. Lindblad, Commun. Math. Phys. **48**, 199 (1976).

[5] A.G. Redfield, Adv. Magn. Reson. **1**, 1 (1965).

[6] M. Goldman, *Quantum Description of High-Resolution NMR in Liquids* (Clarendon Press, Oxford, 1988).

[7] M. Goldman, J. Magn. Reson. **149**, 160 (2001).

[8] J. Cavanagh, W.J. Fairbrother, A.G. Palmer, III, and N.J. Skelton, *Protein NMR Spectroscopy* (Academic Press, New York, 1996).

[9] M. Goldman, J. Magn. Reson. (1969-1992) **60**, 437 (1984).

[10] A. Kumar, R.C.R. Grace, and P.K. Madhu, Prog. Nucl. Magn. Reson. Spectrosc. **37**, 191 (2000).

[11] M.H. Levitt and L. Di Bari, Bull. Magn. Reson. **16**, 94-114 (1994).

[12] G.A. Morris and R. Freeman, J. Am. Chem. Soc. **101**, 760 (1979).

[13] D.P. Burum and R.R. Ernst, J. Magn. Reson. (1969-1992) **39**, 163 (1980).

[14] A.E. Bryson, and Y.C. Ho, *Applied Optimal Control* (Wiley, New York, 1975).